Mechanics Research Communications 131 (2023) 104126

Contents lists available at ScienceDirect

Mechanics Research Communications

journal homepage: www.elsevier.com/locate/mechrescom

Equilibrium and transient response of photo-actuated Liquid Crystal Elastomer beams

Reza Norouzikudiani [a,*], Alessandro Lucantonio [a,c], Antonio DeSimone [a,b]

[a] The BioRobotics Institute, Scuola Superiore Sant'Anna, Viale Rinaldo Piaggio, 34, Pontedera, 56025, Italy
[b] SISSA-Scuola Internazionale Superiore di Studi Avanzati, Trieste, 34136, Italy
[c] Department of Mechanical and Production Engineering, Aarhus University, Inge Lehmanns Gade 10, Aarhus 8000, Denmark

ARTICLE INFO

Keywords:
Liquid crystal elastomers
Light actuation
Photo-chemical strain
Photo-thermal strain
Multi-physics modeling

ABSTRACT

Light actuation is one of the preferred and advantageous approaches to remotely induce and control deformations in soft materials such as photoactive Liquid Crystal Elastomers (LCEs). Various experimental and numerical works have been carried out in the literature to study the actuation of photoactive LCE sheets under illumination. In this study, we have developed a reduced multi-physics model to predict the equilibrium and dynamic response of photoactive LCE beams under illumination. We test our model against an experiment in which a double-clamped thin nematic LCE beam is subjected to UV light, and the stress is generated in the beam due to induced contraction under illumination. Our numerical results demonstrate reasonable agreement with the experiment regarding stress evolution trend and saturation time. We also investigate the bending response of a photoactive LCE beam subjected to UV light. Based on our parameters, we observe that the nematic beam bends towards the light only due to the photochemical strain gradient along the thickness. Finally, to test our model in a dynamic situation, we perform the simulation for the self-oscillations of an LCE beam under illumination. We show that the alternate activation of the top and bottom surfaces of the LCE beam by uniform steady illumination can pump energy into the system, resulting in the phenomenon of self-oscillations.

1. Introduction

Liquid Crystal Elastomers (LCEs) are crosslinked materials with both the elasticity property of polymers and the spontaneous ordering property of liquid crystals (LCs) [1,2]. These materials can switch between anisotropic (nematic) and isotropic states depending on the alignment of the LC molecules. As a result of these characteristics, they can undergo large, spontaneous, and reversible deformations in response to external stimuli such as heat, light, and magnetic fields [2–4]. These properties also make LCEs an attractive candidate for many applications, including soft actuators, artificial muscles, optical devices, and imaging systems [5].

Actuation by light is one of the preferred approaches to induce deformation remotely in LCEs. To make LCEs responsive to light, some dye molecules, such as azobenzene, can be embedded into the polymer backbone [4]. When exposed to UV light, the azobenzene molecules, known as trans isomers in the nematic phase, absorb the light and transform into bent-shaped molecules known as cis isomers. Additionally, the temperature of the sample increases because of the light absorption by trans molecules (direct heating) and thermal recovery of cis isomers (indirect heating). Because of trans-to-cis isomerization, and temperature rise, the liquid crystalline order decreases, leading to a contraction in the alignment direction of the LC mesogens.

Typically, LCEs are synthesized as thin sheets such as beams, plates, and shells. When these sheets are exposed to light, the absorption of light decays as it travels through the thickness of the material. This leads to a non-uniform absorption profile along the thickness, which creates a non-uniform strain field along the thickness. As a result of this strain field, the sheets can undergo dynamic stretching and bending. Specifically, the bending behavior is determined by comparing the thickness to the light decay length. Various experimental studies have been carried out in the literature to exploit these interesting properties of photoactive LCEs and achieve various desired deformation modes. In one of the pioneering works [6], bending deformation is induced along the direction of polarization in the polydomain LCN upon illumination with polarized UV light. The generation of self-excited oscillations under constant external stimuli inspired by biological rhythms such as heartbeat and leaves oscillations [7] can also be observed in photoactive LCE beams. This phenomenon can be observed in thin photoactive nematic LCE beams subjected to light

* Corresponding author.
E-mail address: reza.norouzikudiani@santannapisa.it (R. Norouzikudiani).

https://doi.org/10.1016/j.mechrescom.2023.104126
Received 29 November 2022; Received in revised form 19 April 2023; Accepted 10 May 2023
Available online 13 May 2023

because of photo-chemical effect [8], photo-thermal effect [9], or a combination of both [10,11].

Due to the wide range of potential applications of LCEs, mathematical and numerical models can help us better understand the underlying mechanics that govern the equilibrium and time-dependent responses of LCEs under various external stimuli. There are some theoretical works in the literature that proposed mathematical models based on linear beam theory [12–14] and large deformation theories (without considering inertial terms) [15–18] to predict the equilibrium and transient response of thin LCE beams under light illumination. These studies have often neglected the extensibility of the beam, and considered either the chemical or thermal effect of the illumination in their modeling. Hence, it is still necessary to develop more efficient numerical models based on large deformation theory that consider inertial terms, extensibility of the beam, and both chemical and thermal effects simultaneously to investigate the response of nematic LCE beams under light illumination.

In the present study, we aim to develop a reduced coupled multi-physics model to investigate the static and dynamic response of photoactive nematic thin planar LCE beams under light illumination. In Section 2, we build the model based on the nonlinear rod theory for a planar beam [19], where the internal force and moment at each cross section are derived by considering the thermal and chemical effects of illumination. In Section 3, we perform various numerical simulations to evaluate the capability of our model in different conditions. We test our model against an experimental study [20] in which they have generated the photo stress in a double-clamped photoactive LCE beam under illumination. We also investigate the bending response of nematic photoactive LCE beams subjected to UV light. Finally, we exploit the developed model to generate the self-oscillations phenomenon in a photoactive nematic LCE beam due to alternate activation of both top and bottom surfaces.

2. Mathematical modeling

A thin extensible photoactive beam of length L, thickness h, and width w subjected to illumination with the light intensity $\bar{J}$ is shown in Fig. 1a. The beam is clamped at the left end and has a naturally straight shape in the reference (undeformed) configuration. Also, the beam is in the nematic phase with the alignment direction $\mathbf{n}$, and the light is shined with angle α with respect to the vertical direction. As discussed, upon illumination with UV light on the top surface, light penetrates along the thickness (Fig. 1b), then the trans molecules (n_t) absorb the light, and are isomerized to cis (n_c) molecules (Fig. 1c). Also, the temperature T increases in the sample due to heat generation (Fig. 1d). Because of cis-to-trans conversion (chemical effect) and temperature rise (thermal effect), the order of the liquid crystals is reduced. Therefore, a non-uniform contraction strain field (ε_p) is induced along the alignment's direction $\mathbf{n}$ (Fig. 1e). Due to the presence of ε_p, extensional and bending strains are induced in the beam, which causes the beam to bend towards the light (Fig. 1f).

2.1. Photo induced strain (ε_p)

As explained, the induced photo strain (ε_p) depends on both chemical and thermal effects according to

$$\varepsilon_p = -C_{ch} n_c - C_{th}(T - T_0) \tag{1}$$

where the chemical part is linearly proportional to the fraction of cis molecules [21], and the thermal part is linearly proportional to the difference between current (T) and initial (T_0) temperatures. Also, C_{ch} and C_{th} are positive chemical and thermal coefficients, respectively.

In (1), the fraction of cis molecules is increased by light absorption and decreased by thermal recovery

$$\frac{\partial n_c}{\partial t}(S,z,t) = \Gamma J(S,z,t) n_t(S,z,t) - \frac{n_c(S,z,t)}{\tau} \tag{2}$$

where $n_t = 1 - n_c$ is the fraction of trans molecules, τ denotes the cis life-time (relaxation time back to steady state) and Γ is the material constant that subsumes an absorption cross section per chromophore and a quantum efficiency [22].

Furthermore, the temperature is increased due to heat generation in the sample. We assume that the heat transfer only happens along the thickness. Thus, in order to determine the temperature field $T(S,z,t)$ we use a one-dimensional heat equation

$$\rho c_s \frac{d}{dt} T(S,z,t) - k_a \frac{d^2}{dz^2} T(S,z,t) = H(S,z,t) \tag{3}$$

where c_s is the specific heat coefficient and k_a is the thermal conductivity coefficient. In addition, $H(S,z,t)$ is the rate of heat generation per unit volume of the sample, which depends on both direct (light absorption by trans molecules) and indirect (cis-to-trans conversion) heating

$$H(S,z,t) = \zeta n_t(S,z,t) J(S,z,t) + (U - \Delta)\left(\frac{n_c(S,z,t)}{\tau}\right) \tag{4}$$

In (4), $U - \Delta$ is the released energy per unit volume due to cis-to-trans conversion, and ζ is the material constant.

Finally, in (2) and (4), $J(S,z,t)$ is the amount of light intensity that arrives at each point z along the thickness at time t. In order to compute $J(S,z,t)$, we use the generalized Beer-Lambert law, which represents the light attenuation along the thickness at each cross-section due to photon absorption

$$\frac{\partial J}{\partial z}(S,z,t) = \mathrm{sgn}(\cos(\theta(S,t) + \alpha)) \frac{1 - n_c}{d} J(S,z,t) \tag{5}$$

where d is the penetration depth, and the sign function shows the light path direction across the cross-section.

2.2. Elastodynamics

We utilize the nonlinear Kirchhoff rod theory [19] to describe the mechanical deformations of an extensible planar beam under different types of external stimuli, where the constitutive equations for the internal axial force and moment are derived by considering the induced photo strain (ε_p).

2.2.1. Geometry and kinematics

As shown in Fig. 1f, $\mathbf{r}(S,t)$ indicates the position of each material point S of the mid axis at time t and $\theta(S,t)$ represents the angle between the unit tangent vector $\hat{\mathbf{t}}$ to the mid axis and the horizontal axis $\mathbf{e_1}$. Thus, the unit tangent vector can be described by

$$\hat{\mathbf{t}}(S,t) = \frac{1}{\lambda(S,t)} \frac{\partial \mathbf{r}}{\partial S}(S,t) \tag{6}$$

where $\lambda(S,t) = \frac{ds}{dS} = 1 + \varepsilon(S,t)$ is the axial stretch, and $\varepsilon(S,t)$ denotes the extensional strain of the mid axis. In addition, the bending strain k is defined as the derivative of angle $\theta(S,t)$ with respect to the reference arc length S.

$$k := \frac{\partial \theta}{\partial S}(S,t) \tag{7}$$

2.2.2. Balance of linear and angular momentum

Let $\mathbf{f}(S,t)$ be the resultant internal force and $M(S,t)$ the resultant internal moment at each cross-section. In the absence of external distributed forces and moments, balancing linear and angular momentum yields

$$\frac{\partial \mathbf{f}}{\partial S}(S,t) = \rho A \ddot{\mathbf{r}}(S,t) \tag{8}$$

$$\frac{\partial M}{\partial S}(S,t) + \lambda(S,t)(\hat{\mathbf{t}}(S,t) \times \mathbf{f}(S,t)) \cdot \mathbf{e}_3 = \rho I \ddot{\theta}(S,t) \tag{9}$$

where ρ is the mass density, $A = wh$ is the area of each cross-section, and $I = \frac{wh^3}{12}$ is the second moment of inertia of each cross-section with respect to the mid axis.

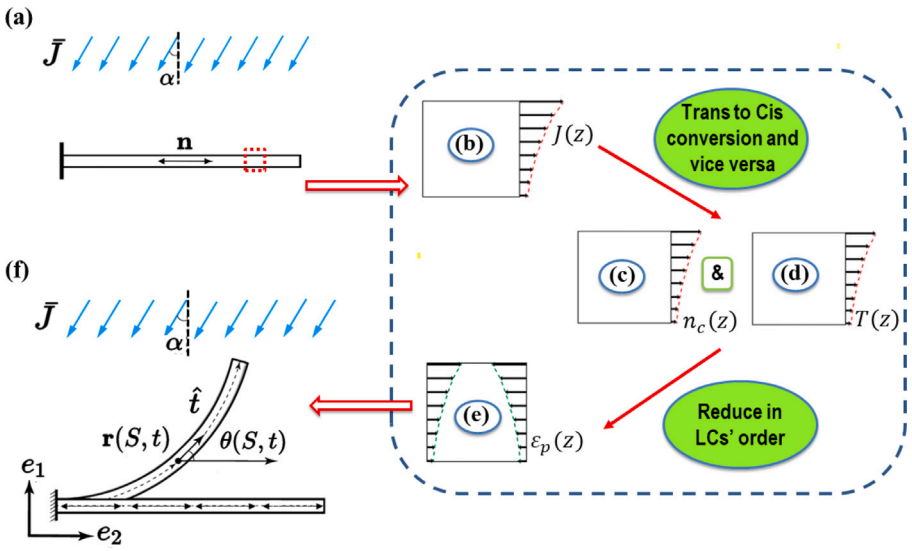

Fig. 1. (a) A thin extensible photoactive nematic beam under illumination in the reference configuration. (b) Upon illumination, light penetrates along the thickness at each cross-section. (c) Then, trans molecules (n_t) absorb light and are converted to cis molecules (n_c). (d) Also, the sample's temperature (T) is increased due to light absorption by trans molecules and cis-to-trans conversion. (e) Due to these chemical and thermal effects, a contraction (ε_p) is induced along the alignment's direction of LCs. (f) Extensional and bending strains are induced in the beam due to the presence of ε_p (current configuration).

Table 1
Mechanical boundary conditions.

Clamped-clamped	Clamped-free
$\theta(0,t)=0$	$\theta(0,t)=0$
$\theta(L,t)=0$	$\mathbf{r}(0,t)=0$
$\mathbf{r}(0,t)=0$	$\mathbf{f}(L,t)=0$
$\mathbf{r}(L,t)=0$	$M(L,t)=0$

2.2.3. Constitutive equations

The constitutive equations for total axial force, $N=\mathbf{f}\cdot\hat{\mathbf{t}}$, and the resultant bending moment, M, at each cross-section are derived by considering the effect of illumination. The axial force N is found by integration of the longitudinal stress field through the thickness

$$N = EA\left(\varepsilon - <\varepsilon_p>\right) \tag{10}$$

where $<()>:=\frac{1}{A}\int_A dA$, and the term $<\varepsilon_p>$ is called the spontaneous extensional strain. Also, E denotes Young's modulus of the LCE sample. In the current study, we neglect the temperature dependence behavior of E and consider it a constant parameter. Then, we derive the constitutive equation for the resultant bending moment by integrating the moment of the stress field with respect to the mid axis over each cross-section

$$M = EI\left(k - \frac{A}{I}<-z\varepsilon_p>\right) \tag{11}$$

where the term $\frac{A}{I}<-z\varepsilon_p>$ is called the spontaneous bending strain. We refer to Appendix A for more information on the derivation of the constitutive Eqs. (10) and (11).

2.3. Boundary conditions

We consider the situations in which the beam is either clamped-clamped or clamped-free (Table 1).

We also assume that the convective heat transfer occurs between the beam's surfaces and the environment. Therefore, the boundary conditions for the heat equation are described by

$$-k_a\frac{\partial T\left(S,\frac{-h}{2},t\right)}{\partial z} = h_c\left[T_{\text{env}} - T\left(S,\frac{-h}{2},t\right)\right] \tag{12}$$

$$-k_a\frac{\partial T\left(S,\frac{h}{2},t\right)}{\partial z} = h_c\left[T\left(S,\frac{h}{2},t\right) - T_{\text{env}}\right] \tag{13}$$

where h_c is the heat convention coefficient, and T_{env} is the environment's temperature. Finally, as shown in Fig. 1f, the boundary condition for Beer–Lambert equation depends on both angles α and θ. The boundary condition for illumination on top surface is described by

$$J(S,\frac{h}{2},t) = \bar{J}\cos(\theta(S,t)+\alpha) \qquad \text{if} \qquad \cos(\theta(S,t)+\alpha)\geq 0 \tag{14}$$

and for illumination on bottom surface is described by

$$J(S,-\frac{h}{2},t) = \bar{J}\cos(\theta(S,t)+\alpha) \qquad \text{if} \qquad \cos(\theta(S,t)+\alpha)< 0 \tag{15}$$

2.4. Numerical aspects

We solve the 11 governing Eqs. (1), (2), (3), (4), (5), (6), (7), (8), (9), (10), and (11) to obtain the unknowns (ε_p, n_c, T, H, J, $\mathbf{r}$, θ, $\mathbf{f}$, M, ε, k). The governing equations are implemented into the finite element software COMSOL Multiphysics v5.6 through the weak form PDE interface Appendix B. The implicit adaptive step-size Generalized Alpha (GA) or BDF solver is used for the time-stepping. A quasi-Newton algorithm is employed to iteratively solve the non-linear algebraic system resulting from the finite element discretization at each time step. The direct solver MUMPS is chosen for the solution of the linearized system at each iteration.

3. Numerical experiments

In this section, we perform various numerical simulations for static and dynamic actuation of thin LCE beams under illumination using the developed multiphysics model. We use the material and geometric properties provided in Table 2 for these simulations. These parameters are extracted from previous experimental and numerical papers [20] except for ζ, C_{th} and C_{ch} that are obtained by fitting the simulation to experimental results. As shown in this table, the lifetime of cis molecules is very high, which allows us to neglect the thermal decay term in (2), and the indirect heating term in (4). In Sections 3.1 and 3.2, we also assume that the deformation caused by illumination takes place over a slow time scale, such that we can neglect the effect of inertia.

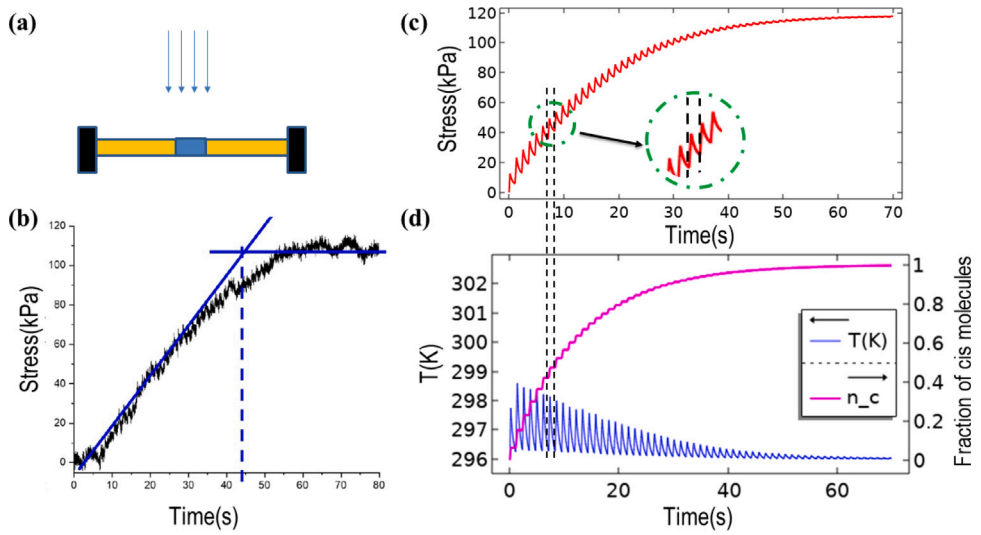

Fig. 2. (a) Schematic of a double-clamped photoactive thin nematic beam under water subjected to the UV light with $40\frac{\text{mW}}{\text{cm}^2}$ intensity. (b) Time evolution of experimentally generated photo stress in the beam; figure reproduced from [20] (c) Time evolution of numericall generated photo stress in the beam (d) Time evolution of the temperature and fraction of cis molecules at a specific cross section ($S = 0.5L$) of the beam.

Table 2
Material and geometric properties of the LCE beam.

Symbol	Definition	Value	Unit
L	Length	5×10^{-3}	m
w	Width	5×10^{-3}	m
h	Thickness	10×10^{-6}	m
E	Young's modulus	100	MPa
ρ	Mass density	1200	Kg/m^3
τ	Cis state lifetime	10^4	s
Γ	Adsorption constant	1×10^{-3}	m^2/J
d	Penetration depth	8×10^{-6}	m
ζ	Material constant	12.5×10^4	1/m
C_{th}	Thermal contraction coefficient	3×10^{-4}	1/K
C_{ch}	Chemical contraction coefficient	8×10^{-3}	
C_s	Specific heat	1666	J/kgK
k_a	Conduction heat coefficient	0.2	W/(mK)
h_c	Convection heat coefficient	25(water) - 5(air)	W/m^{2}K
T_{env}	Environment temperature	296	K
T_0	Initial temperature	296	K

3.1. Photo stress in double-clamped thin LCE beams subjected to UV light

Firstly, we test our model against a recent experimental study [20]. To simulate the experiment, we consider a double-clamped thin nematic beam (Fig. 2a) whose top ($0.45L < S < 0.6L$) is periodically irradiated with light (at each period, the light is on for 200 ms, then off for 1 s). The beam is either immersed in water or surrounded by air. Upon illumination, a contraction (ϵ_p) is induced in the beam and generates stress along the length because of the clamped ends. The time evolution of the experimental [20] and numerical photo stresses in the beam located in water and subjected to the light intensity of $40\frac{\text{mW}}{\text{cm}^2}$ are shown in Fig. 2b and c, respectively. In both the experiment and numerical simulation, the generated photo stress increases with periodic saw tooth profiles due to periodic illumination and is saturated after a transient period. In the transient phase, at each period (Fig. 2c), the stress increases sharply due to the trans-to-cis conversion and the rise in temperature in the presence of light (Fig. 2d). However, when the light is off, due to the lack of illumination, the fraction of cis molecules remains constant and the temperature decreases. Thus, the stress is reduced only because of cooling. After the transient phase, light absorption and heat generation become zero in the beam due to the fact that all trans molecules have been converted to cis molecules. Therefore, the photo stress tends to become a constant (Fig. 2c) because of the saturation of the fraction of cis molecules and the cooling of the beam to its initial temperature (Fig. 2d).

Following the experiment in [20], we also perform simulations for different light intensities and environments. The generated photo stresses in the beam immersed in water for different light intensities (40 and $100\frac{\text{mW}}{\text{cm}^2}$) are shown in Fig. 3a. These results also demonstrate a reasonable agreement with the experiment. According to this figure, increasing the light intensity decreases the stress's saturation time. However, the saturation stress remains constant due to the conversion of all trans molecules to cis molecules under both light intensities. Moreover, the generated photo stress in the beam in both air and water environments subjected to the light intensity of $40\frac{\text{mW}}{\text{cm}^2}$ are shown in Fig. 3b. Unlike the experimental result [20], where the saturated photostress in the air is lower than in water, we obtain the same value in both environments due to the conversion of all trans molecules to cis molecules. One possible cause of this discrepancy is differences in the history of temperatures experienced by the sample in two environments. Temperature effects such as temperature dependence of elastic moduli, or differences in the elastic modulus and the saturated n_c in environments with various initial temperatures, which are discussed in [23], have not been considered in our current modeling. We plan to return to this issue in future work when a more detailed model can be validated against a more comprehensive set of experimental results.

3.2. Bending response of a photoactive nematic beam subjected to UV light

We then use our developed model to investigate the bending response of a photoactive nematic beam under illumination. We consider that the beam is clamped at the left end, and the top surface is illuminated uniformly by steady UV light ($\alpha = 0$). Upon illumination, a gradient photo strain is induced along the beam's thickness, which bends the beam toward the light. However, after some time, the cis molecules profile becomes more uniform along the thickness, which causes the beam to lose its curvature and bend back to its initial configuration (Fig. 4a). Fig. 4b shows the bending deformation of a nematic LCE beam under illumination at time $3s$, considering thermal, chemical, and both effects in (1). Based on our model, the beam does not bend under thermal effect due to the uniform temperature profile along the thickness (Fig. 4c), which generates zero spontaneous bending strain. Thus, the total bending comes only from the chemical effect because of the gradient profile of the fraction of cis molecules (n_c) along the thickness (Fig. 4d). As discussed, with our parameters,

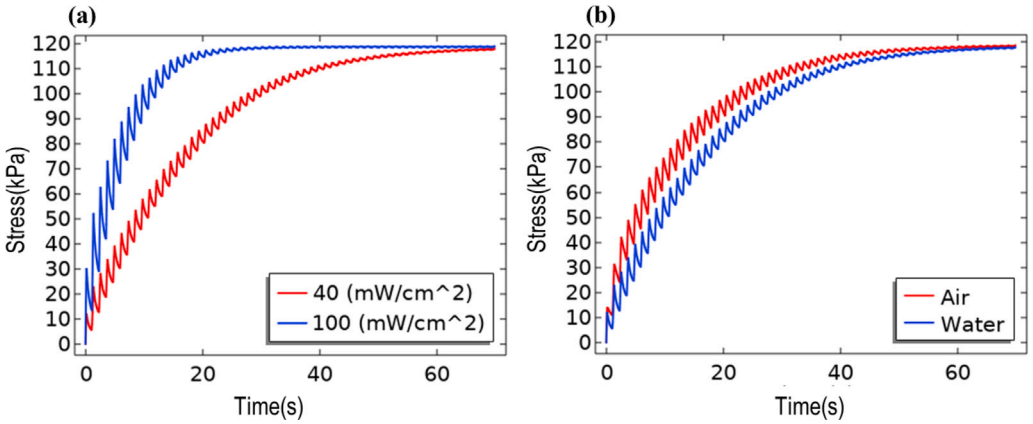

Fig. 3. (a) Photo stress in a double clamped photoactive nematic beam under water subjected to UV light with different intensities (40 and 100 $\frac{mW}{cm^2}$). (b) Photo stress in a double clamped photoactive nematic beam in various environments (air and water) subjected to UV light with 40 $\frac{mW}{cm^2}$ intensity.

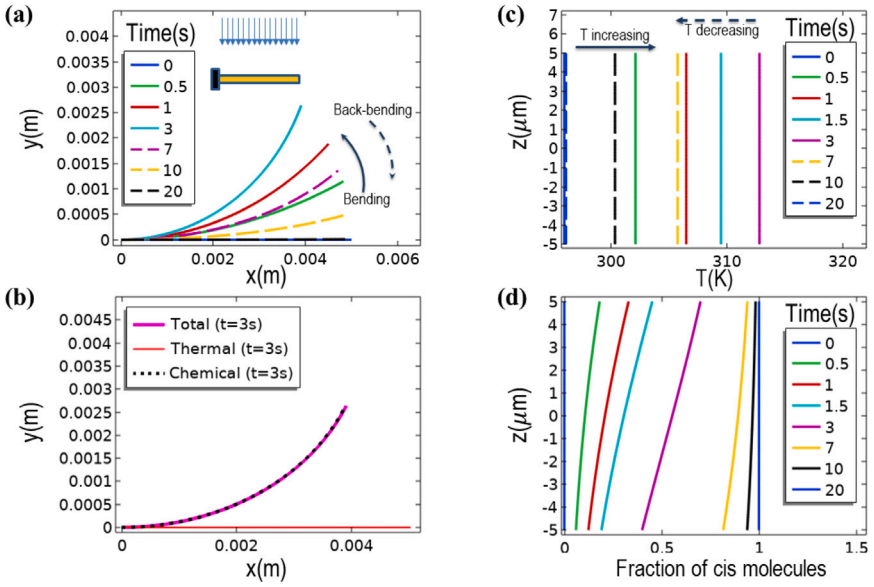

Fig. 4. A clamped-free photoactive nematic beam in air subjected to uniform UV light with 40 $\frac{mW}{cm^2}$ intensity (a) Bending response of the beam over time (b) Bending deformation of the beam at time 3 s due to thermal, chemical, and both effects (c) Temperature profile along the thickness at a specific cross-section ($S = 0.1L$) (d) Fraction of cis molecules (n_c) profile along the thickness at a specific cross-section ($S = 0.1L$).

no bending deformation has been obtained due to the thermal effect. However, varying the parameters like thickness (h), penetration depth (d), light intensity (I), heat conductivity coefficient (k_a), and the heat convection coefficient (h_c) can affect the thermal diffusion in the beam and make the temperature profile non-uniform along the thickness. For instance, in [24,25] the beam's thickness is much greater than our thickness, which can result in a non-uniform temperature profile along the thickness and bending deformation due to the thermal effect.

3.3. Self oscillation due to alternate activation of top and bottom surfaces

In order to evaluate the performance of our model in dynamic situation, we simulate the self-oscillation phenomenon due to alternate activation of the top and bottom surfaces of a thin LCE beam subjected to UV light, inspired by [11]. We assume the beam is clamped at the left side and slightly disturbed due to its weight or a mechanical trigger. Also, the light is shined from the right side ($\alpha = \frac{\pi}{2}$). Unlike [11], in our model the bending oscillation occurs in the beam only due to the chemical effect, as discussed previously. Upon illumination on the top surface, the beam bends toward the light and overshoots its equilibrium state because of its inertia. Then, the bottom surface is illuminated by light (Fig. 5a). Therefore, alternate actuation of the top and bottom surfaces pumps energy into the system (Fig. 5b) and powers self-oscillations (Fig. 5c). However, after some time, the total energy of the system is going to reach a steady state due to the conversion of all trans molecules to cis molecules and increase in the uniformity of spontaneous strain profile along the thickness (Fig. 5d). Since no damping mechanism is included in the model, the stored energy remains constant, which will result in the continued oscillation of the beam with a constant amplitude after the initial growth (Fig. 5e). It is important to note that if damping were included in the model, the stored energy would be dissipated, causing a decrease in the amplitude of oscillation and resulting in the fading away of self-oscillations.

4. Conclusions

In the present study, we developed a one-dimensional model to investigate the equilibrium and transient response of a photoactive nematic thin LCE beam exposed to UV light under different conditions. We built the model based on the nonlinear rod theory for a planar extensible beam where the internal force and moment at each cross-section were derived by considering the photo-induced strain. Also,

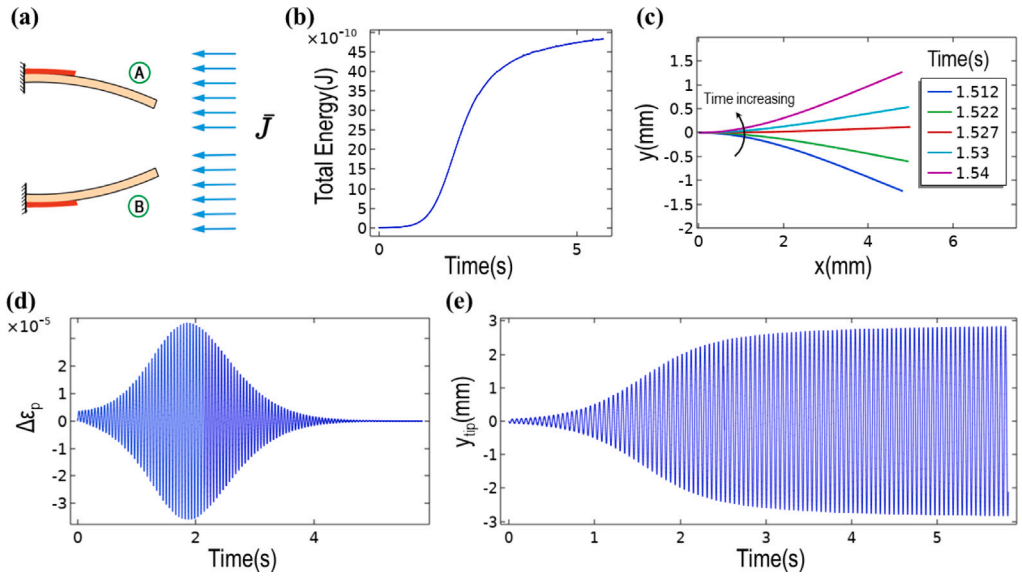

Fig. 5. (a) Schematic of self-oscillation of an LCE beam under illumination with $1000\frac{\text{mW}}{\text{cm}^2}$ light intensity due to alternate actuation of both top and bottom surfaces. The light is shined horizontally from the right side, and we assumed that the beam is perturbed down due to a mechanical trigger before illumination. (b) Variation of total (kinematic and elastic) energy of the LCE beam over time. (c) Snapshot of vibration of the LCE beam under illumination at different time. (d) the evolution of spontaneous strain difference ($\Delta\epsilon_p = \epsilon_p^{top} - \epsilon_p^{bottom}$) over time at a specific cross-section ($S = 0.1L$) (e) Time response of vertical displacement of the beam's tip.

we assumed that thermal and chemical effects were responsible for generating the photo strain in the beam. First, we tested our model against a recent experimental study based on a uni-axial test [20]. We performed simulations for a double-clamped nematic photoactive beam subjected to UV light under different light intensities and environments using the material properties in Table 2. In all conditions, photo stress was generated and increased in the beam due to the trans-to-cis conversion and the rise in temperature, and it was saturated after a transient period when all trans molecules became cis molecules. These results also showed a reasonable agreement with the experiment. Then, we investigated the bending response of a photoactive nematic LCE beam under illumination. Upon illumination, the beam bent toward the light due to the gradient profile of cis molecules along the thickness. However, the beam returned to its initial configuration after some time because of the convertion of all trans molecules to cis molecules. Furthermore, based on our model, we found that bending occurred in the beam only because of the gradient profile of cis molecules along the thickness (chemical effect). Finally, we conducted simulations to test the model in a dynamic situation. We generated self-oscillation in a photoactive nematic beam due to the alternate actuation of both top and bottom surfaces, which pumps energy into the system and powers self-excited oscillation.

Declaration of competing interest

The authors declare the following financial interests/personal relationships which may be considered as potential competing interests: The authors report financial support was provided by European Union's Horizon 2020 Research and Innovation Programme under the Marie Sklodowska-Curie Grant Agreement No. 956150 (STORM-BOTS).

Data availability

Data will be made available on request.

Acknowledgments

We thank the financial support of the European Union's Horizon 2020 Research and Innovation Programme under the Marie Sklodowska-Curie Grant Agreement No. 956150 (STORM-BOTS). We also gratefully acknowledge useful discussions with Hao Zheng, Arri Priimagi, and Peter Palffy-Muhoray. ADS is a member of the INdAM Research Group GNFM.

Appendix A. Derivation of constitutive equations

Since the beam is made of an elastic material and is under illumination, the longitudinal stress (σ) at each point of the cross section is proportional to the elastic strain (ε_{el}), which is the difference between the visible strain (ε_v) and the photo-induced strain (ε_p). Thus, the stress–strain relation is described by

$$\sigma = E\varepsilon_{el} = E\left(\varepsilon_v - \varepsilon_p\right) \tag{A.1}$$

where E denotes Young's modulus of the LCE sample.

Considering the Euler's and Bernoulli's hypothesis, the visible strain ε_v at any point is given by

$$\varepsilon_v = -kz + \varepsilon \tag{A.2}$$

In (A.2), k, ε are the bending and axial strains of the mid axis, respectively. In addition, $\frac{-h}{2} < z < \frac{h}{2}$ is the distance of each fiber from the mid axis.

The total axial force at each cross section is found by integration of stress field through the thickness,

$$N = \int_A \sigma dA = E\int_A \left(\varepsilon_v - \varepsilon_p\right) dA = E\int_A \left(-kz + \varepsilon - \varepsilon_p\right) dA \tag{A.3}$$

Taking the integral in the above equation, we obtain the constitutive equation for the axial force;

$$N = EA\left(\varepsilon - < \varepsilon_p >\right) \tag{A.4}$$

where $< () >:= \frac{1}{A}\int_A dA$, and the term $< \varepsilon_p >$ is called the spontaneous extensional strain. Then, we derive the constitutive equation for the

resultant bending moment by integrating the moment of the stress field with respect to the mid axis over each cross section

$$M = -\int_A \sigma z dA = -E\int_A \left(\varepsilon_v - \varepsilon_p\right) z dA \tag{A.5}$$

which yields the following constitutive law for the bending moment

$$M = EI\left(k - \frac{A}{I} < -z\varepsilon_p >\right) \tag{A.6}$$

In (A.6), the term $\frac{A}{I} < -z\varepsilon_p >$ is called the spontaneous bending strain.

Appendix B. Weak formulations

To solve the governing equations of our coupled multi-physics model using the finite element method, we require to derive their weak forms first. Towards this end, each governing equation (strong form) should be multiplied by an arbitrary test function and integrated over the domains on which they hold. In addition, the order of the spatial derivative are reduced to 1, by implementing integration by parts. Using this approach, the weak forms of Eqs. (2), (3), (5), (7), (8), and (9) are derived.

- Kinematics

$$\int_0^L \tilde{\mathbf{r}}(S,t)\left(\frac{\partial \mathbf{r}}{\partial S}(S,t) - \lambda(S,t)\hat{\mathbf{t}}(S,t)\right) \mathrm{d}S = 0 \tag{B.1}$$

- Equations of motion

$$\int_0^L \tilde{\mathbf{f}}(S,t)\left(\frac{\partial \mathbf{f}}{\partial S}(S,t) - \rho A\ddot{\mathbf{r}}(S,t)\right) \mathrm{d}S = 0 \tag{B.2}$$

$$\int_0^L \left[-\frac{\mathrm{d}\tilde{\theta}}{\mathrm{d}S} M(S,t) - \tilde{\theta}(S,t)\left(\lambda(S,t)(\hat{\mathbf{t}}(S,t)\times \mathbf{f}(S,t))\cdot \mathbf{e}_3 + \rho I\ddot{\theta}(S,t)\right)\right] \mathrm{d}S = 0 \tag{B.3}$$

- Chemical Reaction

$$\int_{\frac{-h}{2}}^{\frac{h}{2}} \tilde{n}_c(S,z,t)\left(\frac{\partial n_c}{\partial t}(S,z,t) - \Gamma J(S,z,t) n_t(S,z,t) + \frac{n_c(S,z,t)}{\tau}\right) \mathrm{d}z = 0 \tag{B.4}$$

- Heat equation

$$\int_{\frac{-h}{2}}^{\frac{h}{2}} \left[k_a \frac{\partial \tilde{T}}{\partial z}(S,z,t)\frac{\partial T}{\partial z}(S,z,t) + \tilde{T}(S,z,t)\left(\rho c_s \frac{\partial T}{\partial t}(S,z,t) - H(S,z,t)\right)\right] \mathrm{d}z - \left[k_a \tilde{T}(S,z,t)\frac{\partial T}{\partial z}(S,z,t)\right]_{-\frac{h}{2}}^{\frac{h}{2}} = 0, \tag{B.5}$$

- Generalized Beer–Lambert law

$$\int_{\frac{-h}{2}}^{\frac{h}{2}} \tilde{J}(S,z,t)\left(\frac{\partial J}{\partial z}(S,z,t) - \mathrm{sgn}(\cos(\theta(S,t)+\alpha))\frac{1-n_c}{d} J(S,z,t)\right) \mathrm{d}z = 0 \tag{B.6}$$

References

[1] P.-G. De Gennes, J. Prost, The Physics of Liquid Crystals, No. 83, Oxford University Press, 1993.

[2] M. Warner, E.M. Terentjev, Liquid Crystal Elastomers, Vol. 120, Oxford University Press, 2007.

[3] F. Kremer, W. Lehmann, H. Skupin, L. Hartmann, P. Stein, H. Finkelmann, Piezoelectricity in ferroelectric liquid crystalline elastomers, Polym. Adv. Technol. 9 (10–11) (1998) 672–676.

[4] H. Finkelmann, E. Nishikawa, G. Pereira, M. Warner, A new opto-mechanical effect in solids, Phys. Rev. Lett. 87 (1) (2001) 015501.

[5] C. Ohm, M. Brehmer, R. Zentel, Applications of liquid crystalline elastomers, Adv. Polym. Sci. 250 (2012) 49–93.

[6] Y. Yu, M. Nakano, T. Ikeda, Directed bending of a polymer film by light, Nature 425 (6954) (2003) 145.

[7] A. Jenkins, Self-oscillation, Phys. Rep. 525 (2) (2013) 167–222.

[8] T.J. White, N.V. Tabiryan, S.V. Serak, U.A. Hrozhyk, V.P. Tondiglia, H. Koerner, R.A. Vaia, T.J. Bunning, A high frequency photodriven polymer oscillator, Soft Matter 4 (9) (2008) 1796–1798.

[9] A.H. Gelebart, G. Vantomme, E. Meijer, D.J. Broer, Mastering the photothermal effect in liquid crystal networks: a general approach for self-sustained mechanical oscillators, Adv. Mater. 29 (18) (2017) 1606712.

[10] K.M. Lee, M.L. Smith, H. Koerner, N. Tabiryan, R.A. Vaia, T.J. Bunning, T.J. White, Photodriven, flexural–torsional oscillation of glassy azobenzene liquid crystal polymer networks, Adv. Funct. Mater. 21 (15) (2011) 2913–2918.

[11] H. Zeng, M. Lahikainen, L. Liu, Z. Ahmed, O.M. Wani, M. Wang, H. Yang, A. Priimagi, Light-fuelled freestyle self-oscillators, Nature Commun. 10 (1) (2019) 1–9.

[12] K. Li, S. Cai, Modeling of light-driven bending vibration of a liquid crystal elastomer beam, J. Appl. Mech. 83 (3) (2016) 031009.

[13] J. Zhao, P. Xu, Y. Yu, K. Li, Controllable vibration of liquid crystal elastomer beams under periodic illumination, Int. J. Mech. Sci. 170 (2020) 105366.

[14] D. Zhao, Y. Liu, A prototype for light-electric harvester based on light sensitive liquid crystal elastomer cantilever, Energy 198 (2020) 117351.

[15] Y. Lin, L. Jin, Y. Huo, Quasi-soft opto-mechanical behavior of photochromic liquid crystal elastomer: Linearized stress–strain relations and finite element simulations, Int. J. Solids Struct. 49 (18) (2012) 2668–2680.

[16] D. Corbett, C. Xuan, M. Warner, Deep optical penetration dynamics in photobending, Phys. Rev. E 92 (1) (2015) 013206.

[17] K. Korner, A.S. Kuenstler, R.C. Hayward, B. Audoly, K. Bhattacharya, A nonlinear beam model of photomotile structures, Proc. Natl. Acad. Sci. 117 (18) (2020) 9762–9770.

[18] A. Goriely, D.E. Moulton, L. Angela Mihai, A rod theory for liquid crystalline elastomers, J. Elasticity (2022) 1–24.

[19] S. Antman, Nonlinear Problems of Elasticity, Springer, 2005.

[20] T. Guo, A. Svanidze, X. Zheng, P. Palffy-Muhoray, Regimes in the response of photomechanical materials, Appl. Sci. 12 (15) (2022) 7723.

[21] D. Corbett, M. Warner, Linear and nonlinear photoinduced deformations of cantilevers, Phys. Rev. Lett. 99 (17) (2007) 174302.

[22] D. Statman, I. Janossy, Study of photoisomerization of azo dyes in liquid crystals, J. Chem. Phys. 118 (7) (2003) 3222–3232.

[23] A. Sánchez-Ferrer, A. Merekalov, H. Finkelmann, Opto-mechanical effect in photoactive nematic side-chain liquid-crystalline elastomers, Macromol. Rapid Commun. 32 (8) (2011) 671–678.

[24] M. Li, S. Lv, J. Zhou, Photo-thermo-mechanically actuated bending and snapping kinetics of liquid crystal elastomer cantilever, Smart Mater. Struct. 23 (12) (2014) 125012.

[25] B. Wu, T. Liu, Y. Chen, L. Jin, Photo-induced spatiotemporal bending of shape memory polymer beams, Smart Mater. Struct. 31 (12) (2022) 125011.